# Rogue-wave solutions of a three-component coupled nonlinear Schrödinger equation

Li-Chen Zhao[1,2] and Jie Liu[1,3,*]

[1]*Science and Technology Computation Physics Laboratory, Institute of Applied Physics and Computational Mathematics, Beijing 100088, China*

[2]*Department of Modern Physics, University of Science and Technology of China, Hefei 230026, China*

[3]*Center for Applied Physics and Technology, Peking University, Beijing 100084, China*

(Received 7 October 2012; revised manuscript received 9 December 2012; published 18 January 2013)

We investigate rogue-wave solutions in a three-component coupled nonlinear Schrödinger equation. With certain requirements on the backgrounds of components, we construct a multi-rogue-wave solution that exhibits a structure like a four-petaled flower in temporal-spatial distribution, in contrast to the eye-shaped structure in one-component or two-component systems. The results could be of interest in such diverse fields as Bose-Einstein condensates, nonlinear fibers, and superfluids.

DOI: 10.1103/PhysRevE.87.013201 PACS number(s): 42.65.Tg, 05.45.−a, 47.20.Ky, 47.35.Fg

## I. INTRODUCTION

A rogue wave (RW) is localized in both space and time and seems to appear from nowhere and disappear without a trace [1,2]. It is one of the most fascinating phenomena in nature and has been observed recently in nonlinear optics [3] and water wave tanks [4]. The studies of RW in single-component systems have indicated that the rational solution of the nonlinear Schrödinger equation (NLS) can be used to describe the phenomenon well [5–8].

A variety of complex systems, such as Bose-Einstein condensates, nonlinear optical fibers, etc., usually involve more than one component [9]. Recent studies are extended to RWs in two-component systems [9–12]. Some new structures such as dark RW have been presented numerically [11] and analytically [12]. Moreover, it was found that two RWs can emerge in the coupled system which are quite distinct from the high-order RW in a one-component system [12]. In the two-component coupled systems, the interaction between a RW and other nonlinear waves is also a hot topic of great interest [9,10,12]. It was shown that a RW attracts a dark-bright wave in Ref. [9].

In the present paper, we further extend the investigation to a three-component coupled system, considering the number of the modes coupled in complex systems is usually more than two. With certain requirements on the backgrounds of components, we construct a new rational solution that can be used to describe the dynamics of single RWs, double RWs, and triple RWs in the system. A structure like a four-petaled flower is found in the coupled system: there are two humps and two valleys around a center in the temporal-spatial distribution, which is quite distinct from the well-known eye-shaped one presented before. We discuss the possibility of observing them in nonlinear fibers.

This paper is organized as follows. In Sec. II, we present exact vector RW solutions and the explicit conditions under which they could exist. Their dynamics are discussed in detail. In Sec. III, the possibility of observing them in a three-mode nonlinear optic fiber is discussed. The conclusions are made in Sec. IV.

*liu_jie@iapcm.ac.cn

## II. EXACT VECTOR ROGUE-WAVE SOLUTIONS

It is well known that coupled NLS equations are often used to describe the interactions among the modes in nonlinear optics, components in BEC, etc. We begin with the well-known three-component coupled NLS, which can be written as

$$\begin{aligned} &i\frac{\partial\psi_1}{\partial t}+\frac{\partial^2\psi_1}{\partial x^2}+2[|\psi_1|^2+|\psi_2|^2+|\psi_3|^2]\psi_1=0,\\ &i\frac{\partial\psi_2}{\partial t}+\frac{\partial^2\psi_2}{\partial x^2}+2[|\psi_1|^2+|\psi_2|^2+|\psi_3|^2]\psi_2=0,\\ &i\frac{\partial\psi_3}{\partial t}+\frac{\partial^2\psi_3}{\partial x^2}+2[|\psi_1|^2+|\psi_2|^2+|\psi_3|^2]\psi_3=0, \end{aligned} \quad (1)$$

where $\psi_j$ $(j=1,2,3)$ represent the wave envelopes, $t$ is the evolution variable, and $x$ is a second independent variable. Equation (1) has been solved to get the vector soliton solution of the trivial background using the Horita bilinear method in Ref. [13]. Performing the Darboux transformation from a trivial seed solution with $\psi_3=0$, one could get the bright-bright solitons in Ref. [14]. It has been reported that solitons could collide inelastically, and there are shape-changing collisions for a coupled system which are different from an uncoupled system [13]. However, it is not possible to study a vector RW with a trivial background. Next, we will solve it with nontrivial seed solutions. The nontrivial seed solutions are derived as follows:

$$\psi_{10}=s_1\exp\left[i2\left(s_1^2+s_2^2+s_3^2\right)t+ik_1x-ik_1^2t\right], \quad (2)$$

$$\psi_{20}=s_2\exp\left[i2\left(s_1^2+s_2^2+s_3^2\right)t+ik_2x-ik_2^2t\right], \quad (3)$$

$$\psi_{30}=s_3\exp\left[i2\left(s_1^2+s_2^2+s_3^2\right)t+ik_3x-ik_3^2t\right], \quad (4)$$

where $s_j$ $(j=1,2,3)$ are arbitrary real constants and denote the backgrounds in which localized nonlinear waves emerge. $k_1$, $k_2$, and $k_3$ denote the wave vectors of the plane wave background in the three components, respectively. From a physical viewpoint, the relative wave vector value is important. One of the three components can be seen as a reference to define the wave vectors of the other two. Then, we can set $k_2=0$ without losing generality. To derive the rational solutions, we find that there are some requirements for the amplitude of each component, and the difference of their wave vectors should be

 

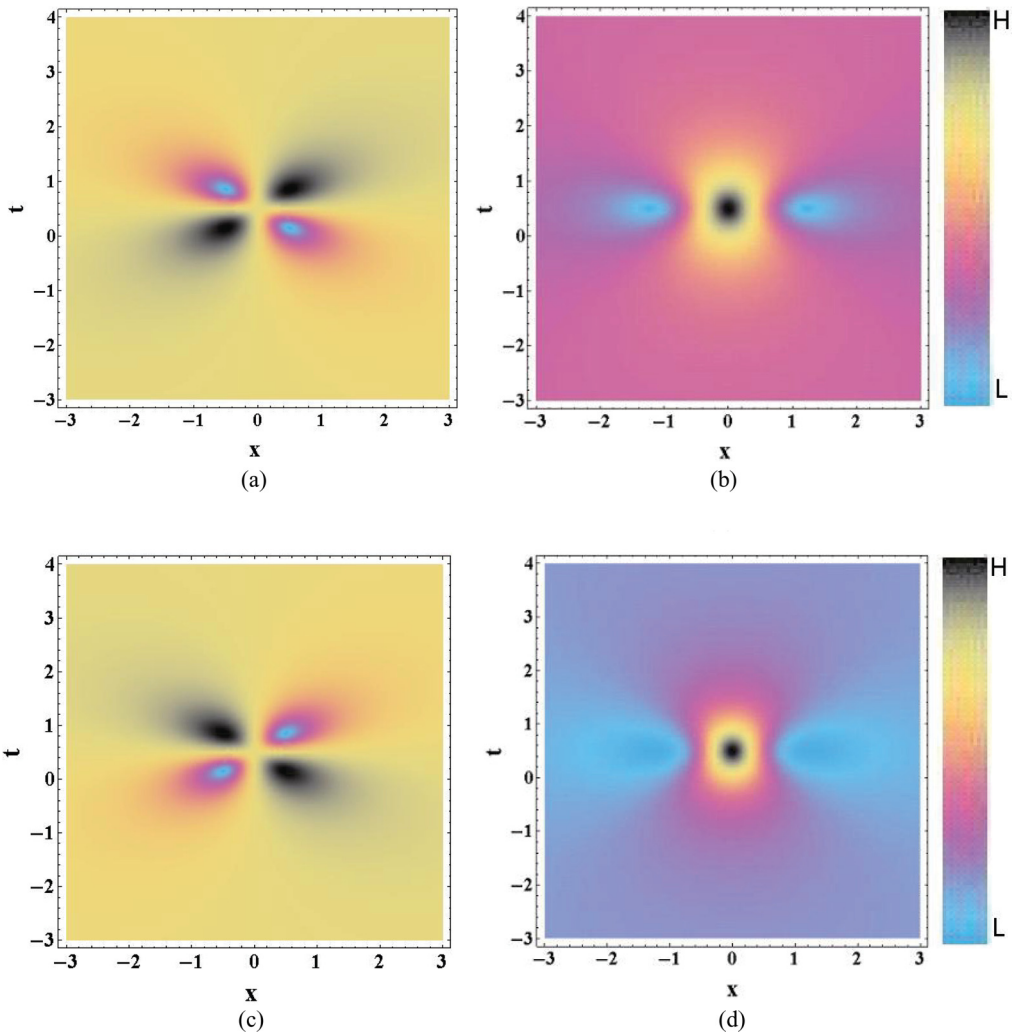


FIG. 1. (Color online) The evolution plot of a single RW in a coupled system (a) for one RW in the $\psi_1$ component, (b) for one RW in the $\psi_2$ component, (c) for one RW in the $\psi_3$ component, and (d) for the whole density of the three components. It is seen that the density distribution shapes of RWs in $\psi_1$ and $\psi_3$ are different from the eye shape. The coefficients are $A_1 = 0, A_2 = 1, A_3 = 0$, and $A_4 = 0$. H and L in the color bar denote high and low values of density, respectively. This holds for all figures.

related to the amplitude in a certain way. The conditions under which one can get vector RWs with no other type of waves are

$$k_1 = -k_3, \quad k_3 = \frac{\sqrt{2}}{2} s_1, \tag{5}$$

$$s_2 = \frac{\sqrt{2}}{2} s_1, \quad s_3 = s_1. \tag{6}$$

With the given conditions and $s_1 = 1$, the generic form of vector RWs could be given as

$$\psi_1 = \left(1 - \frac{H_1(x,t)}{G_1(x,t)}\right) \exp\left[i\frac{9t}{2} - i\frac{x}{\sqrt{2}}\right], \tag{7}$$

$$\psi_2 = \left(1 - \frac{H_2(x,t)}{G_2(x,t)}\right) \frac{\exp[5it]}{\sqrt{2}}, \tag{8}$$

$$\psi_3 = \left(1 - \frac{H_3(x,t)}{G_3(x,t)}\right) \exp\left[i\frac{9t}{2} + i\frac{x}{\sqrt{2}}\right], \tag{9}$$

where $H_j(x,t)$ and $G_j(x,t)$ are given in the Appendix. It is seen that they are all rational forms. In the expressions, $A_j$ ($j = 1,2,3,4$) are arbitrary real parameters. The rational solution can be seen as a vector RW solution, which can be verified by the following RW plots. There are mainly three cases for the generalized vector RW solution.

*Single vector rogue wave*. When $A_3 = 0, A_4 = 0$, there is one RW in each component, as shown in Fig. 1. Interestingly, we find that there is a novel shape for the vector RW solution. The density distribution shapes of the localized waves in $\psi_1$ and $\psi_3$ are quite different from the well-known eye-shaped one. There are two humps and two valleys around a center, and the center's value is almost equal to that of the background, as shown in Figs. 1(a) and 1(c). This structure can be called a four-petaled structure in temporal-spatial distribution. The maximum value of the hump is two times the background's intensity, and the minimum value of the valley is almost zero. Moreover, the humps or valleys in $\psi_1$ correspond to the valleys or humps in $\psi_3$. However, the density distribution in $\psi_2$ is identical to the eye-shaped RW in a single-component system for which there are one hump and two valleys, as shown in

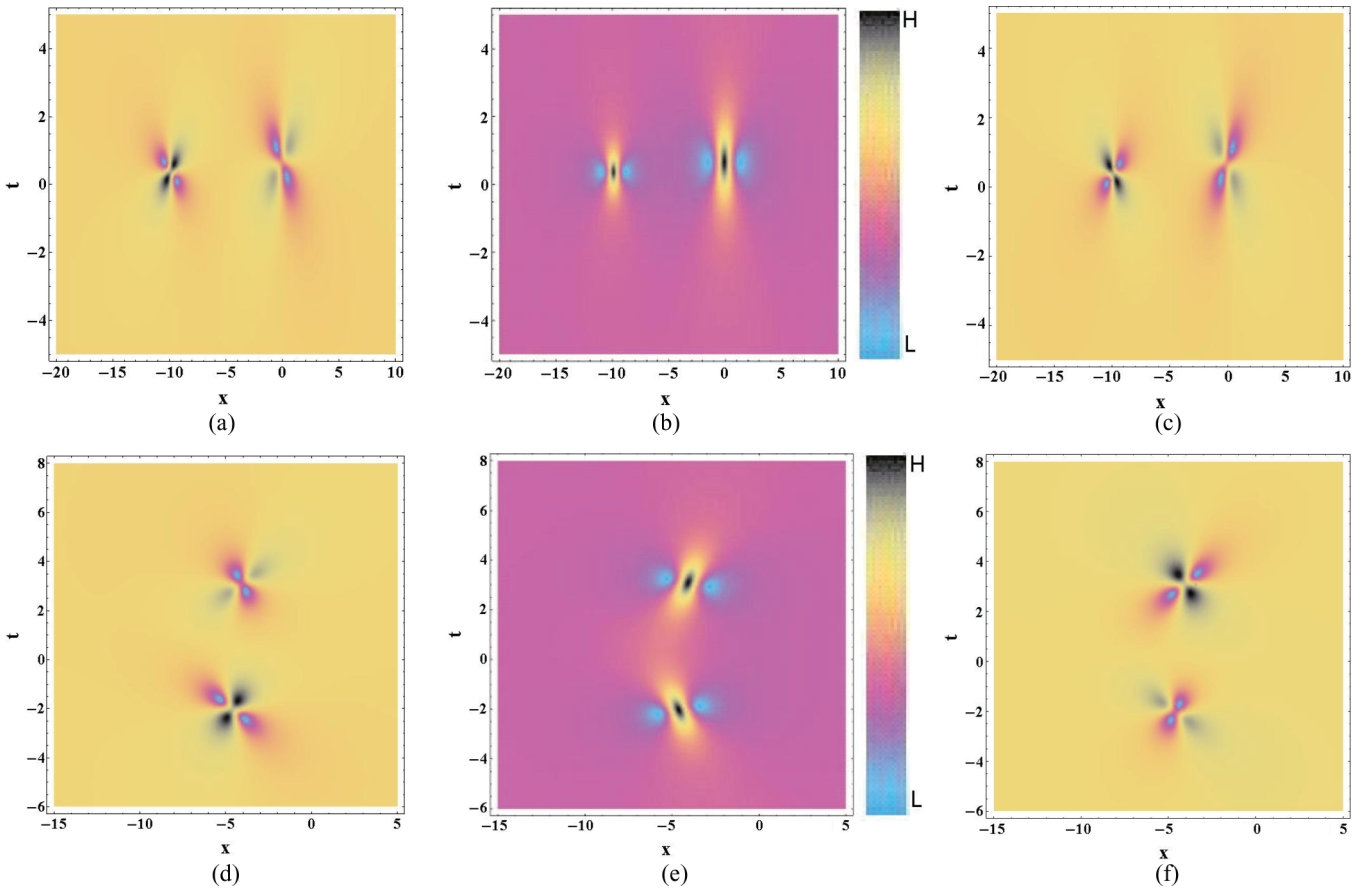


FIG. 2. (Color online) The evolution plot of a double vector RW in a coupled system (a) for the RWs in the $\psi_1$ component, (b) for the RWs in the $\psi_2$ component, and (c) for the RWs in the $\psi_3$ component. The coefficients are $A_1 = 0, A_2 = 40, A_3 = 8$, and $A_4 = 0$. (d), (e), and (f) show the evolution of RWs in $\psi_1$, $\psi_2$, and $\psi_3$, respectively. The coefficients are $A_1 = 150, A_2 = 40, A_3 = 8$, and $A_4 = 0$.

Fig. 1(b). The maximum value of the hump is nine times the background's intensity. Therefore, the whole density is still the well-known eyes shape, as shown in Fig. 1(d). The novel shape should come from the cross-phase modulation effects since the shape cannot be observed in scalar RWs [5,8]. For two-component coupled systems, it has been found numerically that there are dark RWs in one component of the coupled system in Ref. [11]. The dark RW has been given exactly in our previous paper in Ref. [12]. Based on these results, we expect that there should be some novel structures in coupled systems with more than three modes.

*Double vector rogue wave*. When $A_4 = 0$, there are two vector RWs appearing in the temporal-spatial distribution, shown in Fig. 2. When $A_1 \leqslant 0$, there are two vector RWs emerging at a certain time, as shown in Figs. 2(a)–2(c). It is seen that the structures of the two RWs in each mode are similar, and only their sizes are different. The four-petaled RWs emerge in $\psi_{1,3}$ and the eye-shaped ones emerge in $\psi_2$ component. The humps or valleys in $\psi_1$ correspond to the valleys or humps in $\psi_3$. When $A_1 \gg 0$, the two distinct RWs emerge at different times, as shown in Figs. 2(d)–2(f). There is a rotation on the $x$-$t$ distribution plane for the two RWs. Varying the parameter $A_{1,3}$, one can observe the interactions between the two RWs.

*Triple vector rogue wave*. When $A_4 \neq 0$, there are three distinct vector RWs appearing in the temporal-spatial distribution, as shown in Fig. 3. When $A_4 A_2 < 0$ and $|A_2| \gg |A_4|$, there are three vector RWs emerging very clearly at a certain time, as shown in Figs. 3(a)–3(c). Their structures in each component are similar, with different sizes. The humps and valleys in $\psi_1$ still correspond to the valleys and humps in $\psi_3$ component. There are three eye-shaped RWs in $\psi_2$. When $A_4 A_2 > 0$ and $|A_2| \gg |A_4|$, the three RWs emerge clearly at different times, as shown in Figs. 3(d)–3(f). The RW seems to have variable velocity. Varying the parameters, we can investigate the interaction between these vector RWs conveniently. For example, making $A_2$ approach $A_4$, we can observe the interaction of the three RWs, such as in Fig. 4, which shows that a RW's shape can be changed greatly through interacting with others. Two RWs almost fuse to one valley in the $\psi_3$ component with the condition, as shown in Fig. 4(c).

It should be noted that the distribution shapes of the double and triple RWs in the whole temporal-spatial distribution are very distinct from the high-order RW in a one-component system presented in [8,15,16]. In the one-component systems, it is not possible to observe just two RWs appearing in the whole temporal-spatial distribution, even for high-order RWs. Three RWs can emerge in the temporal-spatial distribution for a second-order scalar RW [15], but their distribution shapes are different from the triple vector RWs obtained here.

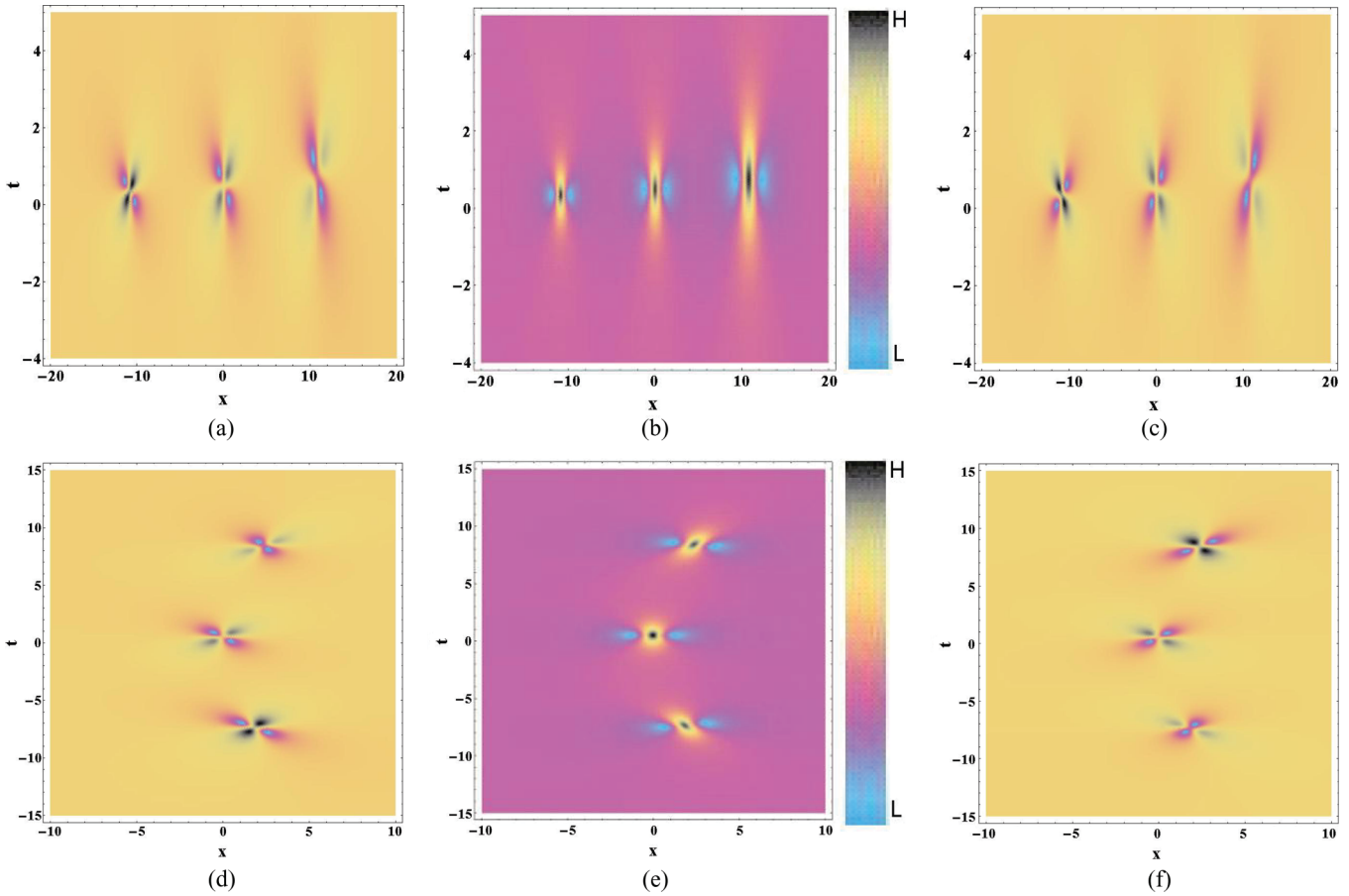


FIG. 3. (Color online) The evolution plot of triple vector RWs in a coupled system (a) for the RWs in the $\psi_1$ component, (b) for the RWs in the $\psi_2$ component, and (c) for the RWs in the $\psi_3$ component. The coefficients are $A_1 = 0, A_2 = 20, A_3 = 0$, and $A_4 = -1$. (d), (e), and (f) show the evolution of RWs in $\psi_1$, $\psi_2$, and $\psi_3$, respectively. The coefficients are $A_1 = 0, A_2 = 20, A_3 = 0$, and $A_4 = 1$.

## III. APPLICATION TO A NONLINEAR OPTIC FIBER SYSTEM

The coupled system discussed above can be used to describe many physical systems, such as a three-component BEC, multimode optical transmission, and so on [17–21]. As an example, here we discuss a possible way to observe the vector RWs in a three-mode nonlinear optic fiber system.

For nonlinear optic fibers, the coordinates $x$ and $t$ above denote the retarded time and propagation distance, respectively. The second derivative coefficients in Eq. (1) correspond to group velocity dispersion (GVD) effects, and the nonlinear coefficients correspond to self-phase modulation and cross-phase modulation effects [18]. Recently, a scalar RW has been realized with an anomalous GVD regime in a one-mode nonlinear fiber [3]. Therefore, one could introduce three-mode optical signals into a nonlinear fiber in the anomalous GVD regime, marked by $\psi_j$ ($j = 1,2,3$), to observe the vector RW presented here. When the operation wavelength of each mode is nearly 1.55 $\mu$m, the GVD coefficient will be $-20$ ps$^2$ km$^{-1}$ in the anomalous regime, and the Kerr coefficients are nearly 1.1 W$^{-1}$ km$^{-1}$, corresponding to the self-focusing effect in the fiber [22]. The unit in $x$ direction will be denoted as 0.23 ps, and the one in $t$ will be denoted as 0.55 km. The backgrounds on which the vector RW can be exited can be given by Eqs. (5) and (6). Explicitly, the background power intensity of $\psi_1$ is set to be 30 W, the background power of $\psi_2$ is 15 W, and the background power of $\psi_3$ is 30 W. The frequency $k_2$ of $\psi_2$ is set to be $\frac{c\ \mu\text{m ps}^{-1}}{1.55\ \mu\text{m}}$ ($c$ is the velocity of light in the fiber), and the frequencies of $\psi_1$ and $\psi_3$ are $k_1 = k_2 - \sqrt{15}\ ps^{-1}$ and $k_3 = k_2 + \sqrt{15}\ ps^{-1}$. Then the initial optical signals can be given by the presented vector RW solution, Eqs. (7)–(9), including density and phase forms. Under the corresponding conditions, single, double, and triple vector RWs could be observed in the nonlinear fiber. For example, the single vector RW can be obtained with $A_3 = 0, A_4 = 0$. From the above studies, we can know that the maximum intensity value in $\psi_{1,3}$ is 60 W, and the maximum intensity in $\psi_2$ is 135 W.

## IV. CONCLUSION

In summary, we investigate rogue-wave solutions in a three-component coupled nonlinear Schrödinger equation using the Darboux transformation method. We find some novel spatial temporal structures for single, double, and triple vector RWs in the coupled system. The corresponding conditions for their emergence are presented explicitly. The coupled system can be used to describe three-component BECs, multimode optical transmission, and so on. As an example, we have discussed the possible way to observe the vector RWs in the physical system of three-mode nonlinear optic fibers.

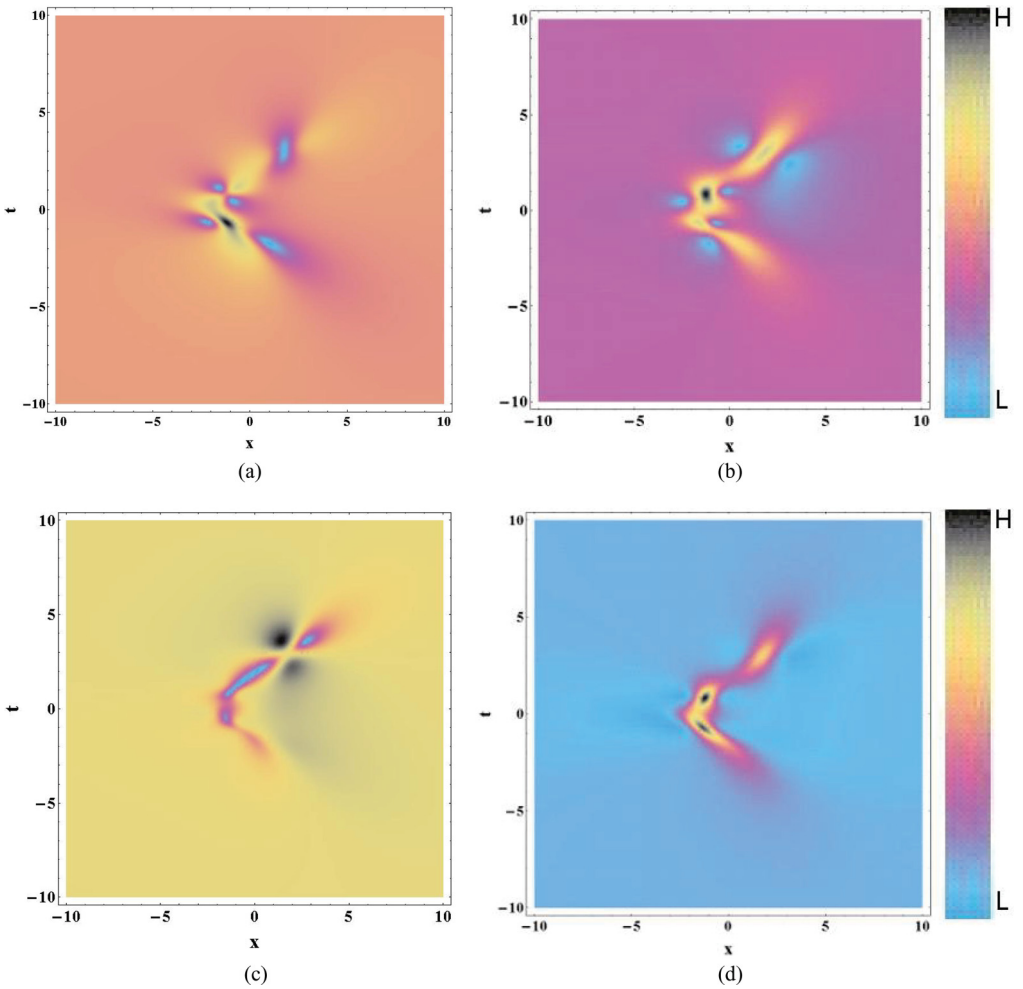


FIG. 4. (Color online) The interaction plot of a triple RW in the coupled system (a) for the RWs in the $\psi_1$ component, (b) for the RWs in the $\psi_2$ component, (c) for the RWs in the $\psi_3$ component, and (d) for the whole density of the three components. The coefficients are $A_1 = 0, A_2 = 1, A_3 = 1$, and $A_4 = 1$.


## ACKNOWLEDGMENTS

This work is supported by the National Fundamental Research Program of China (Contract No. 2011CB921503) and the National Science Foundation of China (Contracts No. 11274051 and No. 91021021).


## APPENDIX: THE EXPLICIT EXPRESSIONS FOR $H_j(x,t)$ AND $G_j(x,t)$

The expressions of $H_j(x,t)$ and $G_j(x,t)$ in Eqs. (7)–(9) are

$$\begin{aligned}
H_1 &= (8-8i)\sqrt{2}A_4^2\,t^6 - (48-24i)\sqrt{2}A_4^2\,t^5 + B_{14}\,t^4 \\
&\quad + B_{13}\,t^3 + B_{12}\,t^2 + B_{11}\,t + B_{10} \\
&\quad + \sqrt{2}(1-i)A_4^2\,x^6 + 6\left[\sqrt{2}A_3A_4(1-i) - A_4^2\right]x^5 \\
&\quad + C_{14}(t)\,x^4 + C_{13}(t)\,x^3 + C_{12}(t)\,x^2 + C_{11}(t)\,x, \\
G_1 &= 8\sqrt{2}A_4^2\,t^6 - 24\sqrt{2}A_4^2\,t^5 + D_{14}\,t^4 \\
&\quad + D_{13}\,t^3 + D_{12}\,t^2 + D_{11}\,t + D_{10} \\
&\quad + \sqrt{2}A_4^2\,x^6 + 6\sqrt{2}A_3A_4\,x^5 \\
&\quad + E_{14}(t)\,x^4 + E_{13}(t)\,x^3 + E_{12}(t)\,x^2 + E_{11}(t)\,x, \\
H_2 &= 16A_4^2\,t^6 - (48+48i)A_4^2\,t^5 + B_{24}\,t^4 + B_{23}\,t^3 \\
&\quad + B_{22}\,t^2 + B_{21}\,t + B_{20} \\
&\quad + 2A_4^2\,x^6 + 12A_3A_4\,x^5 + C_{24}(t)\,x^4 \\
&\quad + C_{23}(t)\,x^3 + C_{22}(t)\,x^2 + C_{21}(t)\,x, \\
G_2 &= 8A_4^2\,t^6 - 24A_4^2\,t^5 + D_{24}\,t^4 \\
&\quad + D_{23}\,t^3 + D_{22}\,t^2 + D_{21}\,t + D_{20} \\
&\quad + A_4^2\,x^6 + 6A_3A_4\,x^5 + E_{24}(t)\,x^4 \\
&\quad + E_{23}(t)\,x^3 + E_{22}(t)\,x^2 + E_{21}(t)\,x, \\
H_3 &= (8+8i)\sqrt{2}A_4^2\,t^6 - 24i\sqrt{2}A_4^2\,t^5 + B_{34}\,t^4 + B_{33}\,t^3 \\
&\quad + B_{32}\,t^2 + B_{31}\,t + B_{30} \\
&\quad + (1+i)\sqrt{2}A_4^2\,x^6 + 6[(1+i)\sqrt{2}A_3 - A_4]A_4\,x^5 \\
&\quad + C_{34}(t)\,x^4 + C_{33}(t)\,x^3 + C_{32}(t)\,x^2 + C_{31}(t)\,x, \\
G_3 &= 8\sqrt{2}A_4^2\,t^6 - 24\sqrt{2}A_4^2\,t^5 + D_{34}\,t^4 \\
&\quad + D_{33}\,t^3 + D_{32}\,t^2 + D_{31}\,t + D_{30} \\
&\quad + \sqrt{2}A_4^2\,x^6 + 6\sqrt{2}A_3A_4\,x^5 + E_{34}(t)\,x^4 \\
&\quad + E_{33}(t)\,x^3 + E_{32}(t)\,x^2 + E_{31}(t)\,x.
\end{aligned}$$

The expressions for $B_{ji}$, $D_{ji}$, $C_{ji}(t)$, and $E_{ji}(t)$ are given as follows:

$$\begin{aligned}
B_{14} &= (12-12i)\big[3\sqrt{2}A_3^2 - 4\sqrt{2}A_2A_4 - (9+i)A_3A_4 \\
&\quad + (13+7i)\sqrt{2}A_4^2\big], \\
B_{13} &= 24i\big\{(3+6i)\sqrt{2}A_3^2 - (2+12i)A_3A_4 \\
&\quad - \sqrt{2}A_4[(4+8i)A_2 + (7-10i)A_4]\big\}, \\
B_{12} &= (36+36i)\big[-2i\sqrt{2}A_2^2 + 2i\sqrt{2}A_1A_3 \\
&\quad - (1-5i)A_2A_3 + (4-5i)\sqrt{2}A_3^2 \\
&\quad + (1-5i)A_1A_4 - (4-4i)\sqrt{2}A_2A_4 \\
&\quad - (5-i)A_3A_4 + (2+4i)\sqrt{2}A_4^2\big], \\
B_{11} &= 72\big[(-2+i)\sqrt{2}A_2^2 + (2-i)\sqrt{2}A_1A_3 \\
&\quad + (2+i)A_2A_3 - (1+2i)\sqrt{2}A_3^2 - (2+i)A_1A_4 \\
&\quad + (2+2i)\sqrt{2}A_2A_4 - 2A_3A_4 + \sqrt{2}A_4^2\big], \\
B_{10} &= (36-36i)\big\{\sqrt{2}A_1^2 + (1+i)\sqrt{2}A_2^2 \\
&\quad + 2A_2A_3 + (1-i)\sqrt{2}A_2A_4 \\
&\quad - (1+i)A_1[A_2 + \sqrt{2}A_3 + (1-i)A_4]\big\}, \\
C_{14}(t) &= (9-9i)\sqrt{2}A_3^2 + 6\sqrt{2}A_4[(2-2i)A_2 + A_4] \\
&\quad - 30A_3A_4 - (12-6i)\sqrt{2}A_4^2\,t + (6-6i)\sqrt{2}A_4^2\,t^2, \\
C_{13}(t) &= 12\big\{-3A_3^2 + A_2[(3-3i)\sqrt{2}A_3 - 4A_4] \\
&\quad + 2\sqrt{2}A_3A_4 + (1-i)A_4(\sqrt{2}A_1 + 2A_4)\big\} \\
&\quad + 24A_4[(-2+i)\sqrt{2}A_3 + (2+i)A_4]t \\
&\quad + 24[(1-i)\sqrt{2}A_3 - (3-2i)A_4]A_4\,t^2, \\
C_{12}(t) &= 36\big[(1-i)\sqrt{2}A_2^2 + (1-i)\sqrt{2}A_1A_3 - 3A_2A_3 \\
&\quad + \sqrt{2}A_3^2 - A_1A_4 + (2-2i)A_3A_4 - i\sqrt{2}A_4^2\big] \\
&\quad + 36\big[(-2+i)\sqrt{2}A_3^2 + (4+2i)A_3A_4 - 2i\sqrt{2}A_4^2\big]t \\
&\quad + (36-36i)\big[\sqrt{2}A_3^2 - (5+i)A_3A_4 \\
&\quad + (3+2i)\sqrt{2}A_4^2\big]t^2 \\
&\quad - (48-24i)\sqrt{2}A_4^2\,t^3 + (12-12i)\sqrt{2}A_4^2\,t^4, \\
C_{11}(t) &= -72\big\{A_2^2 + A_1[(-1+i)\sqrt{2}A_2 + A_3 + \sqrt{2}A_4] \\
&\quad - \sqrt{2}A_2A_3 + iA_3[(1+i)A_3 + \sqrt{2}A_4]\big\} \\
&\quad + 72\big\{(-2+i)\sqrt{2}A_2A_3 + (2+i)A_3^2 - 2i\sqrt{2}A_3A_4 \\
&\quad + [(2-i)\sqrt{2}A_1 - 2A_4]A_4\big\}t \\
&\quad - 72i\big\{(1+i)\sqrt{2}A_2A_3 + (1+5i)\sqrt{2}A_3A_4 \\
&\quad - (2+3i)A_3^2 + A_4[(-1-i)\sqrt{2}A_1 + (2-3i)A_4]\big\}t^2 \\
&\quad + 48A_4[(-2+i)\sqrt{2}A_3 + (6-i)A_4]t^3 \\
&\quad + 24[(1-i)\sqrt{2}A_3 - (5-4i)A_4]A_4\,t^4, \\
D_{14} &= 12\big[3\sqrt{2}A_3^2 - 8A_3A_4 + \sqrt{2}A_4(-4A_2 + 9A_4)\big], \\
D_{13} &= -24\big[3\sqrt{2}A_3^2 - 4A_3A_4 + \sqrt{2}A_4(-4A_2 + A_4)\big], \\
D_{12} &= 36\big(2\sqrt{2}A_2^2 - 2\sqrt{2}A_1A_3 + 3\sqrt{2}A_3^2 + 4A_1A_4 \\
&\quad - 2A_3A_4 - 2A_2(2A_3 + \sqrt{2}A_4)\big], \\
D_{11} &= -72\sqrt{2}\big(A_2^2 - A_1A_3\big), \\
D_{10} &= 18\big(2\sqrt{2}A_1^2 + 2\sqrt{2}A_2^2 + 4A_2A_3 + 2\sqrt{2}A_3^2 \\
&\quad + 2\sqrt{2}A_2A_4 + 6A_3A_4 + 3\sqrt{2}A_4^2\big), \\
E_{14}(t) &= 3\sqrt{2}\big[3A_3^2 + A_4(4A_2 + 3A_4)\big] \\
&\quad - 6\sqrt{2}A_4^2\,t + 6\sqrt{2}A_4^2\,t^2, \\
E_{13}(t) &= 12\{A_4[\sqrt{2}A_1 + 3(\sqrt{2}A_3 + A_4)] \\
&\quad + 3\sqrt{2}A_2A_3\} - 24\sqrt{2}A_3A_4\,t \\
&\quad + 24(\sqrt{2}A_3 - 2A_4)A_4\,t^2, \\
E_{12}(t) &= 18\big(2\sqrt{2}A_2^2 + 2\sqrt{2}A_1A_3 + 2\sqrt{2}A_3^2 + 2\sqrt{2}A_2A_4 \\
&\quad + 6A_3A_4 + 3\sqrt{2}A_4^2\big) - 36\sqrt{2}A_3^2\,t \\
&\quad + 36\big(\sqrt{2}A_3^2 - 4A_3A_4 + 2\sqrt{2}A_4^2\big)\,t^2 \\
&\quad - 24\sqrt{2}A_4^2\,t^3 + 12\sqrt{2}A_4^2\,t^4, \\
E_{11}(t) &= 36\big[2\sqrt{2}A_1A_2 + 2A_3^2 + 3\sqrt{2}A_3A_4 + 3A_4^2 \\
&\quad + 2A_2(\sqrt{2}A_3 + A_4)\big] + 72\sqrt{2}(-A_2A_3 + A_1A_4)\,t \\
&\quad + 72\big[\sqrt{2}A_2A_3 - 2A_3^2 + 2\sqrt{2}A_3A_4 \\
&\quad - A_4(\sqrt{2}A_1 + A_4)\big]\,t^2 + 48A_4(-\sqrt{2}A_3 + 2A_4)\,t^3 \\
&\quad + 24(\sqrt{2}A_3 - 4A_4)A_4\,t^4, \\
B_{24} &= 24\big\{3A_3^2 - 4\sqrt{2}A_3A_4 \\
&\quad + A_4[-4A_2 + (4+5i)A_4]\big\}, \\
B_{23} &= -48\big\{(3+3i)A_3^2 - (2+2i)\sqrt{2}A_3A_4 \\
&\quad - A_4[(4+4i)A_2 + (4+i)A_4]\big\}, \\
B_{22} &= 72\big[2A_2^2 - 2A_1A_3 - 2\sqrt{2}A_2A_3 \\
&\quad + 3iA_3^2 + 2\sqrt{2}A_1A_4 + (2-4i)A_2A_4 \\
&\quad - \sqrt{2}A_3A_4 + (2-5i)A_4^2\big], \\
B_{21} &= -72\big[(2+2i)A_2^2 - (2+2i)A_1A_3 - (3+i)A_3^2 \\
&\quad + (4+2i)A_2A_4 - (2+i)\sqrt{2}A_3A_4 + 2A_4^2\big], \\
B_{20} &= 72\big[A_1^2 + iA_2(A_2 + \sqrt{2}A_3 + 2A_4) \\
&\quad + (1-i)A_1(A_3 + \sqrt{2}A_4)\big], \\
C_{24}(t) &= 6\big\{3A_3^2 + A_4[4A_2 + (2+i)A_4]\big\} \\
&\quad - (12+12i)A_4^2\,t + 12A_4^2\,t^2, \\
C_{23}(t) &= 12\big[2A_1A_4 + (4+2i)A_3A_4 + (1+2i)\sqrt{2}A_4^2 \\
&\quad + 6A_2A_3\big] - (48+48i)A_3A_4\,t \\
&\quad + 48A_4(A_3 - \sqrt{2}A_4)\,t^2, \\
C_{22}(t) &= 36\big[2A_2^2 + 2A_1A_3 + (1+i)A_3^2 + 2A_2A_4 \\
&\quad + (1+2i)\sqrt{2}A_3A_4 + 2iA_4^2\big] \\
&\quad + 72\big[(-1-i)A_3^2 + A_4^2\big]\,t \\
&\quad + 72\big[A_3^2 - 2\sqrt{2}A_3A_4 + (1+i)A_4^2\big]\,t^2 \\
&\quad - (48+48i)A_4^2\,t^3 + 24A_4^2\,t^4,
\end{aligned}$$

$$
\begin{aligned}
C_{21}(t) &= 72\{A_1[2A_2+(1-i)A_4]+iA_3(\sqrt{2}A_3+2A_4)\\
&\quad +A_2[(1+i)A_3+\sqrt{2}A_4]\}\\
&\quad -72\{-A_4\big[(2+2i)A_1+2A_3+(2+i)\sqrt{2}A_4\big]\\
&\quad +(2+2i)A_2A_3\}\,t+72[2A_2A_3-2\sqrt{2}A_3^2\\
&\quad +(2+2i)A_3A_4-A_4(2A_1+\sqrt{2}A_4)]t^2\\
&\quad +(96+96i)A_4(-A_3+\sqrt{2}A_4)\,t^3\\
&\quad +48A_4(A_3-2\sqrt{2}A_4)\,t^4,\\
D_{24} &= 12\big[3A_3^2-4\sqrt{2}A_3A_4+A_4(-4A_2+9A_4)\big],\\
D_{23} &= -24\big[3A_3^2-2\sqrt{2}A_3A_4+A_4(-4A_2+A_4)\big],\\
D_{22} &= 36\big[2A_2^2-2A_1A_3+3A_3^2+2\sqrt{2}A_1A_4\\
&\quad -\sqrt{2}A_3A_4-2A_2(\sqrt{2}A_3+A_4)\big],\\
D_{21} &= 72\big(-A_2^2+A_1A_3\big),\\
D_{20} &= 18\big[2A_1^2+2A_2^2+2A_3^2+3\sqrt{2}A_3A_4\\
&\quad +3A_4^2+2A_2(\sqrt{2}A_3+A_4)\big],\\
E_{24}(t) &= 9A_3^2+3A_4(4A_2+3A_4)-6A_4^2\,t+6A_4^2\,t^2,\\
E_{23}(t) &= 6[6A_2A_3+A_4(2A_1+6A_3+3\sqrt{2}A_4)]\\
&\quad -24A_3A_4\,t+24A_4(A_3-\sqrt{2}A_4)\,t^2,\\
E_{22}(t) &= 18\big(2A_2^2+2A_1A_3+2A_3^2+2A_2A_4\\
&\quad +3\sqrt{2}A_3A_4+3A_4^2\big)-36A_3^2\,t\\
&\quad +36\big(A_3^2-2\sqrt{2}A_3A_4+2A_4^2\big)\,t^2\\
&\quad -24A_4^2\,t^3+12A_4^2\,t^4,\\
E_{21}(t) &= 18\big(4A_1A_2+4A_2A_3+2\sqrt{2}A_3^2+2\sqrt{2}A_2A_4\\
&\quad +6A_3A_4+3\sqrt{2}A_4^2\big)+72(-A_2A_3+A_1A_4)\,t\\
&\quad +36\big[2A_2A_3-2\sqrt{2}A_3^2-A_4(2A_1+\sqrt{2}A_4)\\
&\quad +4A_3A_4\big]t^2+48A_4(-A_3+\sqrt{2}A_4)\,t^3\\
&\quad +24A_4(A_3-2\sqrt{2}A_4)\,t^4,\\
B_{34} &= (12+12i)\big\{3\sqrt{2}A_3^2-(9-i)A_3A_4\\
&\quad +2\sqrt{2}A_4[-2A_2+(4-i)A_4]\big\},\\
B_{33} &= -24i\big[3\sqrt{2}A_3^2-6A_3A_4+\sqrt{2}A_4(-4A_2+3A_4)\big],\\
B_{32} &= (36+36i)\big[2\sqrt{2}A_2^2-2\sqrt{2}A_1A_3-(5-i)A_2A_3\\
&\quad +(2-i)\sqrt{2}A_3^2+(5-i)A_1A_4-(1-i)A_3A_4\big],\\
B_{31} &= -72i\big[\sqrt{2}A_2^2-A_2A_3+A_1(-\sqrt{2}A_3+A_4)\big],\\
B_{30} &= (36+36i)A_1[\sqrt{2}A_1-(1-i)A_2],\\
C_{34}(t) &= (3+3i)\big[3\sqrt{2}A_3^2+4\sqrt{2}A_2A_4-(5-5i)A_3A_4\big]\\
&\quad -6i\sqrt{2}A_4^2\,t+(6+6i)\sqrt{2}A_4^2\,t^2,\\
C_{33}(t) &= 12\big[(3+3i)\sqrt{2}A_2A_3+(1+i)\sqrt{2}A_1A_4\\
&\quad -3A_3^2-4A_2A_4\big]-24i(\sqrt{2}A_3-A_4)A_4\,t\\
&\quad +24[(1+i)\sqrt{2}A_3-(3+2i)A_4]A_4\,t^2,\\
C_{32}(t) &= 36\big[(1+i)\sqrt{2}A_2^2+(1+i)\sqrt{2}A_1A_3\\
&\quad -3A_2A_3-A_1A_4\big]-36iA_3(\sqrt{2}A_3-2A_4)\,t\\
&\quad +(36+36i)\big[\sqrt{2}A_3^2-(5-i)A_3A_4\\
&\quad +(2-i)\sqrt{2}A_4^2\big]t^2\\
&\quad -24i\sqrt{2}A_4^2t^3+(12+12i)\sqrt{2}A_4^2t^4,\\
C_{31}(t) &= 72\big[(1+i)\sqrt{2}A_1A_2-A_2^2-A_1A_3\big]\\
&\quad -72i\big(\sqrt{2}A_2A_3-A_3^2-\sqrt{2}A_1A_4\big)\,t\\
&\quad +72\big\{(1+i)\sqrt{2}A_2A_3+(3+i)\sqrt{2}A_3A_4\\
&\quad -(3+2i)A_3^2-A_4[(1+i)\sqrt{2}A_1+A_4]\big\}t^2\\
&\quad -48i(\sqrt{2}A_3-3A_4)A_4\,t^3\\
&\quad +24[(1+i)\sqrt{2}A_3-(5+4i)A_4]A_4\,t^4,\\
D_{34} &= 12\big[3\sqrt{2}A_3^2-8A_3A_4+\sqrt{2}A_4(-4A_2+9A_4)\big],\\
D_{33} &= -24\big[3\sqrt{2}A_3^2-4A_3A_4+\sqrt{2}A_4(-4A_2+A_4)\big],\\
D_{32} &= 36\big[2\sqrt{2}A_2^2-2\sqrt{2}A_1A_3+3\sqrt{2}A_3^2+4A_1A_4\\
&\quad -2A_3A_4-2A_2(2A_3+\sqrt{2}A_4)\big],\\
D_{31} &= -72\sqrt{2}\big(A_2^2-A_1A_3\big),\\
D_{30} &= 18\big(2\sqrt{2}A_1^2+2\sqrt{2}A_2^2+4A_2A_3+2\sqrt{2}A_3^2\\
&\quad +2\sqrt{2}A_2A_4+6A_3A_4+3\sqrt{2}A_4^2\big),\\
E_{34}(t) &= 3\sqrt{2}\big[3A_3^2+A_4(4A_2+3A_4)\big]\\
&\quad -6\sqrt{2}A_4^2\,t+6\sqrt{2}A_4^2\,t^2,\\
E_{33}(t) &= 12\{3\sqrt{2}A_2A_3+A_4[\sqrt{2}A_1+3(\sqrt{2}A_3+A_4)]\}\\
&\quad -24\sqrt{2}A_3A_4\,t+24(\sqrt{2}A_3-2A_4)A_4\,t^2,\\
E_{32}(t) &= 18\big(2\sqrt{2}A_2^2+2\sqrt{2}A_1A_3+2\sqrt{2}A_3^2+2\sqrt{2}A_2A_4\\
&\quad +6A_3A_4+3\sqrt{2}A_4^2\big)-36\sqrt{2}A_3^2\,t\\
&\quad +36\big(\sqrt{2}A_3^2-4A_3A_4+2\sqrt{2}A_4^2\big)\,t^2\\
&\quad -24\sqrt{2}A_4^2\,t^3+12\sqrt{2}A_4^2\,t^4,\\
E_{31}(t) &= 36\big[2\sqrt{2}A_1A_2+2A_3^2+3\sqrt{2}A_3A_4+3A_4^2\\
&\quad +2A_2(\sqrt{2}A_3+A_4)\big]+72\sqrt{2}(-A_2A_3+A_1A_4)\,t\\
&\quad +72\big[\sqrt{2}A_2A_3-2A_3^2+2\sqrt{2}A_3A_4\\
&\quad -A_4(\sqrt{2}A_1+A_4)\big]t^2\\
&\quad +48A_4(-\sqrt{2}A_3+2A_4)\,t^3\\
&\quad +24(\sqrt{2}A_3-4A_4)A_4\,t^4.
\end{aligned}
$$


[1] N. Akhmediev, J. M. Soto-Crespo, and A. Ankiewicz, Phys. Lett. A **373**, 2137 (2009).

[2] C. Kharif and E. Pelinovsky, Eur. J. Mech. B **22**, 603 (2003).

[3] D. R. Solli, C. Ropers, P. Koonath, and B. Jalali, Nature (London) **450**, 06402 (2007); B. Kibler, J. Fatome, C. Finot, G. Millot, F. Dias, G. Genty, N. Akhmediev, and J. M. Dudley, Nat. Phys. **6**, 790 (2010).

[4] A. Chabchoub, N. P. Hoffmann, and N. Akhmediev, Phys. Rev. Lett. **106**, 204502 (2011).
[5] A. Ankiewicz, J. M. Soto-Crespo, and N. Akhmediev, Phys. Rev. E **81**, 046602 (2010).
[6] N. Akhmediev, A. Ankiewicz, and M. Taki, Phys. Lett. A **373**, 675 (2009).
[7] V. V. Voronovich, V. I. Shrira, and G. Thomas, J. Fluid Mech. **604**, 263 (2008).
[8] N. Akhmediev, A. Ankiewicz, and J. M. Soto-Crespo, Phys. Rev. E **80**, 026601 (2009).
[9] F. Baronio, A. Degasperis, M. Conforti, and S. Wabnitz, Phys. Rev. Lett. **109**, 044102 (2012).
[10] B. L. Guo and L. M. Ling, Chin. Phys. Lett. **28**, 110202 (2011).
[11] Y. V. Bludov, V. V. Konotop, and N. Akhmediev, Eur. Phys. J. Spec. Top. **185**, 169 (2010).
[12] L. C. Zhao and J. Liu, J. Opt. Soc. Am. B **29**, 3119 (2012).
[13] M. Vijayajayanthi, T. Kanna, and M. Lakshmanan, Phys. Rev. A **77**, 013820 (2008); Eur. Phys. J. Spec. Top. **173**, 57 (2009).
[14] L. C. Zhao and S. L. He, Phys. Lett. A **375**, 3017 (2011).
[15] B. L. Guo, L. M. Ling, and Q. P. Liu, Phys. Rev. E **85**, 026607 (2012).
[16] Y. Ohta and J. K. Yang, Proc. R. Soc. A **468**, 1716 (2012).
[17] C. Cambournac, T. Sylvestre, H. Maillotte, B. Vanderlinden, P. Kockaert, Ph. Emplit, and M. Haelterman, Phys. Rev. Lett. **89**, 083901 (2002).
[18] A. Hasegawa, Opt. Lett. **5**, 416 (1980).
[19] P. Das, T. S. Raju, U. Roy, and Prasanta K. Panigrahi, Phys. Rev. A **79**, 015601 (2009).
[20] C. Becker, S. Stellmer, P. S. Panahi, S. Dorscher, M. Baumert, E.-M. Richter, J. Kronjager, K. Bongs, and K. Sengstock, Nat. Phys. **4**, 496 (2008).
[21] C. Hamner, J. J. Chang, P. Engels, and M. A. Hoefer, Phys. Rev. Lett. **106**, 065302 (2011); M. A. Hoefer, J. J. Chang, C. Hamner, and P. Engels, Phys. Rev. A **84**, 041605(R) (2011).
[22] J. M. Dudley, G. Genty, F. Dias, B. Kibler, and N. Akhmediev, Opt. Express **17**, 21497 (2009).